MANSOURA JOURNAL OF GEOLOGY
Official Journal of Faculty of Science, Mansoura University, Egypt
E-mail: scimag@mans.edu.eg ISSN: 1687-5087

Using Airborne Gamma-Ray spectrometric data for delineation of radioactive zones in Hamash Area, Southeastern Desert, Egypt

Hatem Aboelkhair[1], Islam Abou El-Magd[2] Hamdy Seisa[3], Maged Mamdouh[3]
[1]Damietta University, Faculty of Science, Geology Department, New Damietta, Egypt
[2]National Authority for Remote Sensing and Space Sciences, Cairo, Egypt
[3]Mansoura University, Faculty of Science, Geology Department, Mansoura, Egypt

Received:1/9/2019
Accepted: 25/9/2019

Abstract: Hamash area is located in the South Eastern Desert of Egypt which covers an area of approximately 2,000 Km^2. The geologic outcrops of the area display a wide range of stratigraphic rock units from Precambrian to Quaternary. The main goal of this paper is to use gamma-ray spectrometric data for delineation of radioelement concentration in Hamash area, Southeastern Desert, Egypt. Airborne Gamma-ray spectrometric data has been used to detect and highlight the main radioactive zones, and to reveal the relationship between airborne radioactive detected zones and their different types of related geologic units. The radioelement concentration values of the equivalent Uranium (eU), equivalent Thorium (eTh), and Potassium (K) successively discriminated several distinctive radioactive zones over Hamash area. Gamma-ray spectrometric data shows distinct values and responses for the alteration zones around the gold mines in the Hamash area and within different rock types which may be considered new host rocks of gold mineralization.

keywords: Gamma-ray, Gold Mineralization, Eastern Desert, Egypt.

1.Introduction

single alpha or beta decay with specific energy distinguishing the parent nucleus. Consequently, if the energy of a gamma-ray is detected, its emitter can be deduced. In practice, each radionuclide has its particular fingerprint. The radioactive elements in the bedrock have vanished as the formation of the rocks, and only K^{40}, U^{235}, U^{238} and Th^{232} are long-lived enough to be more or less abundant in the earth materials. In airborne gamma-ray spectrometry, three windows are used to record the radiation emitted by K^{40}, $U^{238,}$ and Th^{232} [15]. The gamma-ray spectrometry method has been commonly used in geological mapping [3];[4];[13];[17], mineral exploration [1];[11];[14];[19], soil mapping [6];[21] and in observing the environmental radiation [12];[18];[20]. The gamma-ray spectrometric method measures the radioactive elements, (U), thorium (Th) and potassium (K) those existing in the top surface of the earth's crust where the soil profiles and the rock-forming minerals occur. The radiometric method has individualities compared with other geophysical tools, first of all, the recorded

The study area is located in the Southern portion of the Eastern Desert of Egypt (Fig.1). The area is bordered by latitude 24°29'36.49"N and 24°49'53.49"N and longitude 33°46'20.87"E and 34°19'33.17"E. It is located about 64 kilometers south from the city of Marsa Alam and about 92 Kilometers of Edfu city with an area of about 2000 km^2. The geologic outcrops of the area display a wide range of stratigraphic rock units from Precambrian to Quaternary.

Airborne gamma-ray spectrometry is a passive remote sensing technique that records the naturally radiated gamma radiation radiated from the three radioelements, i.e., potassium, uranium, and thorium, exist in soils and rocks located within the upper 30 cm of the earth's surface [9]; [5]. The use of gamma-ray spectrometry as a tool for geological mapping, environmental monitoring and exploring radioelement concentrations has found widespread acceptance over several decades and continues to be developed [16]. The gamma-ray spectrometry is based on the departure of gamma rays from the nucleus after

with elevations ranging between 785 and 231 meters .

Stratigraphically, the study area consists of foreland sediments represented by the Cretaceous and Tertiary Formations as well as Quaternary deposits filling wadis and their streams plus the huge plains which situated between high lands, these sedimentary rocks overlying Precambrian rocks. The diversities of rocks types are displaying in the geological map of the area (Fig.2)]7[. Precambrian rocks cover the central and eastern parts of the study area and consist of a ring complex, meta-volcanic, meta-sediments, (meta-gabbro)-(meta-diorite) complex, leucocratic and melanocratic medium to high grade metamorphic rocks, ophiolites, gneisses, calc-alkaline granites (older and younger), Dokhan volcanic, and upper Cretaceous volcanic (wadi Natash volcanic) and trachyte plugs. Meanwhile, the upper Cretaceous sedimentary rocks cover most of the western part of the study area and comprise of the Abu Aggag, Umm Barmil, Taref, and Quseir Formations .

Structurally, the study area subjected to different tectonic movements giving rise to some complex structures, and it cut up by many types of faults and joints, which are associated with wadis (dry valleys) and drainage lines or cutting through country rocks (Fig.2)

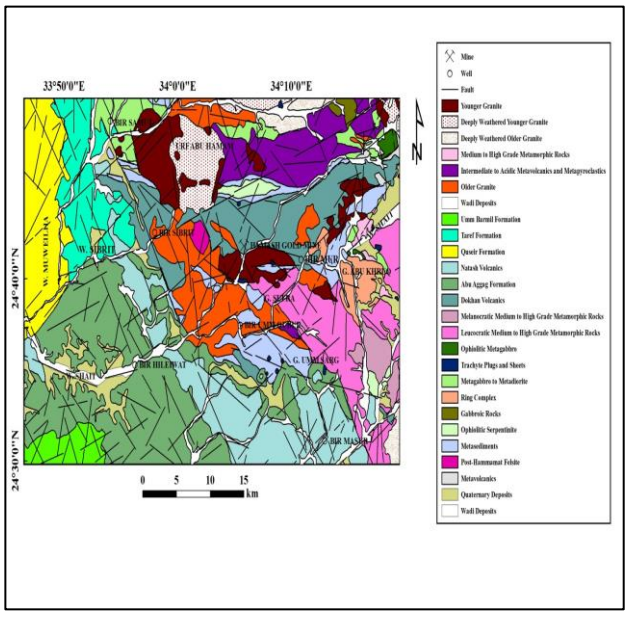

Fig. (2) Geologic map of Hamash area, South Eastern Desert, Egypt, modified after Conoco, 1987.

.Data and Methods

radioactivity radiated from only a few centimeters on the top of the earth's surface with Poverty in the possibility to reveal the subsurface geology compared with other geophysical methods those explore the subsurface geology. Secondly, radiometric data are used for mapping the change in chemical than the physical properties of the survey area [8]. The main objective of this study is the detection and mapping of radioactive anomalies in Hamash Area, Southeastern Desert, Egypt

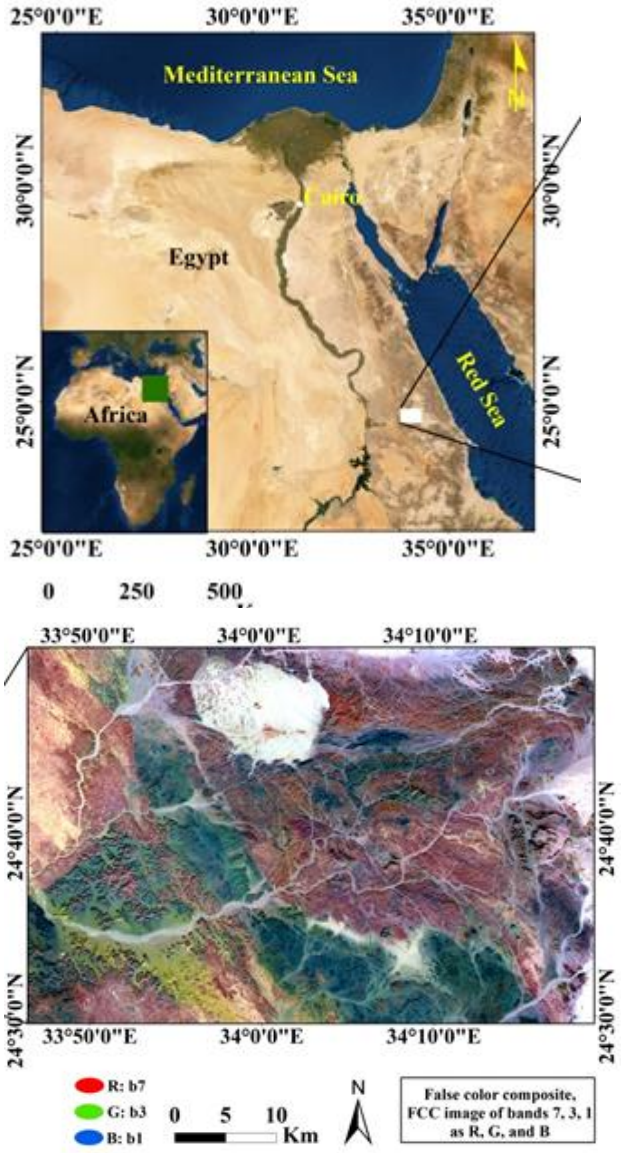

Fig. (1) Location map of Hamash area, South Eastern Desert, Egypt

Geological Setting

The area under investigation is a part of the Pan African Arabian–Nubian Shield that was discussed by several workers. Topographically, the Hamash area is a low mountainous area

The total count map (TC) (Fig. 3) can be divided into three zones of high radioactivity; the first zone is recorded in the north direction of the map which associated with younger granite, metagabbro to metadiorite and Post Hammamat felsite. The second one is recorded in NW-SE trending direction and is associated with Natash Volcanics Abu Aggag formation and Taref formation. The third one is recorded in the eastern side of the map and is associated with the younger granite, older granite, leucocratic medium to high-grade metamorphic rocks, trachyte plugs and sheets, and ring complex (Fig.3). There are two high gamma-ray anomalies in the northeast corner and the southwest corner of the map which associated with younger granite and Quaternary deposits respectively. Also in the northern part of the map, there are high to moderate gamma-ray levels and associated with intermediate to acidic metavolcanics and metapyroclastics rocks. gabbroic rocks record moderate values (Fig. 3).

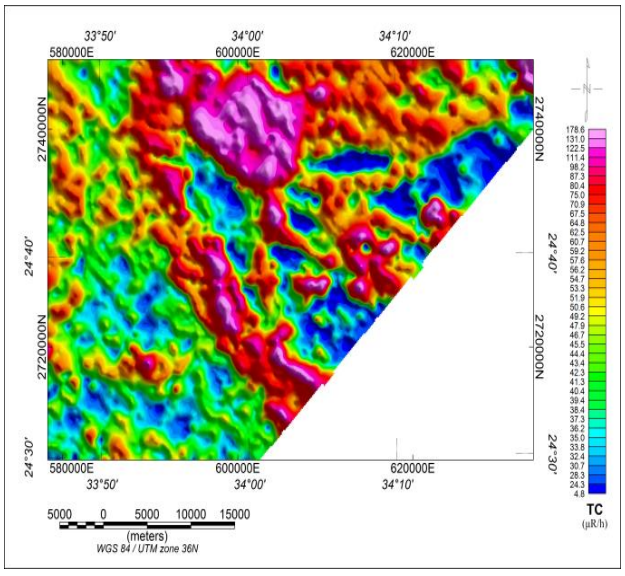

Fig. (3) Total count map in µR/h, of Hamash area, South Eastern Desert, Egypt

Radioelement maps

The equivalent uranium map (eU)

The equivalent uranium map (eU) (Fig.4) similar to the total count map (TC) unless the northwestern side of the map and can be divided into four zones of high gamma-ray radioactivity, the first zone is recorded in the north direction of the map which associated with younger granite, some parts of metagabbro to metadiorite and Post Hammamat felsite (Fig. 4). The second one is recorded in NW-SE

Hamash area was involved in the airborne gamma-ray spectrometric survey performed by Aero Service Division, Western Geophysical Company of America, in 1984 over a large region of the central and southern Eastern Desert, Egypt]2[. The survey was flown along with a set of parallel traverse flight lines oriented in a NE-SW direction, at 1.5 km spacing, whereas tie lines were flown NW-SE at 10 km intervals and 120-m terrain clearance. A high-sensitivity 256-channel airborne gamma-ray spectrometer was used to operate the gamma-ray spectrometric survey (Aero-Service 1984). The acquired airborne gamma-ray spectrometric data were collected and displayed in the form of contoured maps of scale1:500000. The gamma-ray measurements were: 1) corrected for background radiation produced from cosmic rays and aircraft contamination, differences caused by variations in aircraft altitude relative to the ground and Compton scattered gamma-rays in potassium and uranium energy windows, then collected and presented in the form of contour maps]2[. These maps display the apparent surface concentrations of radioelement Potassium (K in %), equivalent Uranium (eU in ppm), equivalent Thorium (eTh in ppm) and Total count Total counts were measured in count per second (cps) and then converted into micro Roentgen per hour (µR/h). 2) geo-referencing the map sheets for each element to UTM (Universal Traverse Mercator) system 3) Gridding each element using minimum curvature tool. The preprocessing stages for aerospectrometric data organized using Oasis Montaj 8.3 package software.

2. Result and discussion

The airborne gamma-ray spectrometry images provide assessments of the overall concentration of elements and generally comprise concentration related to various lithologies. The data include the total count (TC) in µR/h, equivalent uranium (eU) in ppm, equivalent thorium (eTh) in ppm, and potassium concentration (K %). These data were used to build four radioelements image maps (Tc, eU, eTh, and K) and ternary (composite) images in Hamash area .

The total count map (TC)

the Cretaceous formations (Umm Barmil formation, Taref formation, and Quseir formation) and Quaternary deposits. There are high gamma-ray levels observed in the northeastern extreme part of the map which associated with younger granite, and moderate levels observed in the northeast part of the map and are associated with intermediate to acidic metavolcanics and metapyroclastics rocks.

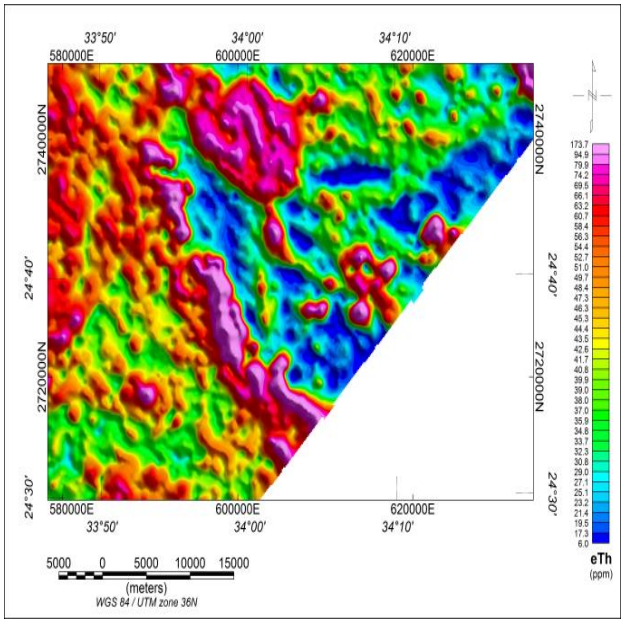

Fig. (5) Equivalent thorium map in ppm, of Hamash area, South Eastern Desert, Egypt

The potassium map (K)

The potassium map (K) (Fig. 6) can also be divided into three zones of high radioactivity; the first zone is recorded in the north direction of the map which associated with younger granite, metagabbro to metadiorite and Post Hammamat felsite (Fig. 6). The second one is recorded in NW-SE trending direction which represents high to moderate radioactivity and is associated with Natash Volcanics, Abu Aggag formation, and older granite (Fig. 6). The third one is recorded in the eastern side of the map and is associated with the younger granite, older granite, leucocratic medium to high-grade metamorphic rocks, trachyte plugs and sheets, and ring complex (Fig. 6). There are high gamma-ray levels observed in northern and northeastern parts of the map which associated with intermediate to acidic metavolcanics and metapyroclastics, and metagabbro to metadiorite, northeastern extreme part of the map and associated with gabbroic rocks and younger granite, and in the southwestern part of the map and is associated with Quaternary trending direction and is associated with Natash Volcanics Abu Aggag formation and Taref formation. The third one is recorded in the eastern side of the map and is associated with the younger granite, older granite, leucocratic medium to high-grade metamorphic rocks, trachyte plugs and sheets, and ring complex and the fourth one is recorded in the northwestern side of the map and is associated with Taref formation and Quseir formation (Fig. 4.(

There are high gamma-ray levels which associated with Quaternary deposits and Um Barmil formation in the southwestern part, intermediate to acidic metavolcanics and metapyroclastics rocks in the northeastern part and younger granite in the northeastern extreme part (Fig. 4).

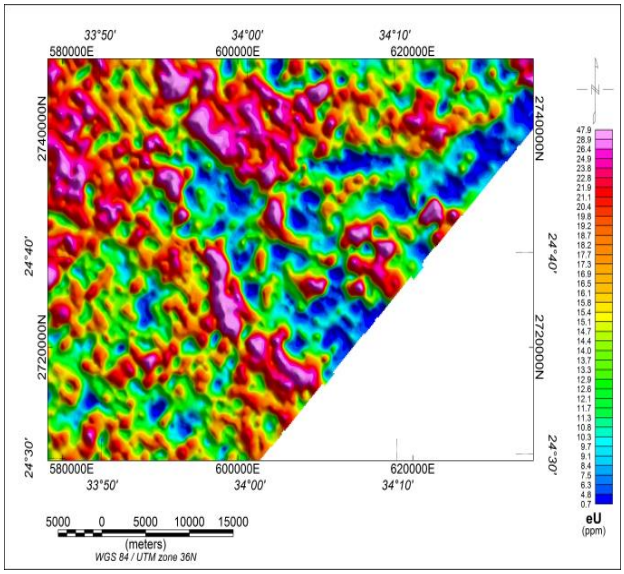

Fig. (4) Equivalent uranium map in ppm, of Hamash area, South Eastern Desert, Egypt.

The equivalent thorium map (eTh)

The equivalent thorium map (eTh) (Fig. 5) can be divided into three zones of high radioactivity; the first zone is recorded in the north direction of the map which associated with younger granite, metagabbro to metadiorite and Post Hammamat felsite (Fig. 5). The second one is recorded in NW-SE trending direction and is associated with Natash Volcanics and Abu Aggag formation (Fig. 5). The third one is recorded in the eastern side of the map and is associated with the younger granite, older granite, leucocratic medium to high-grade metamorphic rocks, trachyte plugs and sheets, and ring complex (Fig. 5). There are high gamma-ray levels observed in some western parts of the map which associated with

The thorium composite image combines eTh (in red) with two ratios eTh/eU (in green) and eTh/K (in blue) (Fig. 7). This image highlights the relative distribution of thorium and emphasizes zones of thorium enrichment. Owing to the map the high concentration of eTh is associated with intermediate to acidic metavolcanics and metapyroclastics, vary from moderate to low values in Cretaceous formations (Abu Aggag formation, Umm Barmil formation, Taref formation, and Quseir formation). The high concentration of eTh, eTh/eU, eTh/K is marked by the white color and generally it is limited in two rock units they are older granite, leucocratic medium to high-grade metamorphic rocks, Quaternary deposits and Abu Aggag formation (Fig. 7). On the other hand, the low concentration of eTh, eTh/eU, eTh/K is marked by the dark color and mainly it is limited in the basement rocks particularly in Dokhan volcanics, older granite, ophiolitic serpentinite, and intermediate to acidic metavolcanics and metapyroclastics (Fig. 7). The high eTh/eU ratio appears in green color and is associated with the basement rocks, in the sedimentary rocks there are some green color spots of moderately high eTh/eU ratio which associated with Taref formation and Abu Aggag formation (Fig. 7). eTh/K ratio appears in blue color and its value is very high in basement rocks which appears with dark blue color and is associated with Dokhan volcanics, ophiolitic serpentinite, younger granite, and older granite. On the other hand, the eTh/K ratio displays moderate values in sedimentary rocks particularly in Cretaceous formations (Abu Aggag formation, Umm Barmil formation, and Taref formation).

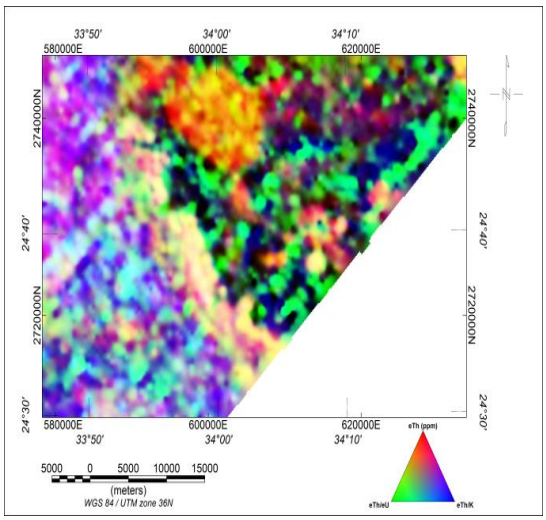

deposits. The very low values of gamma-ray were observed in ophiolitic serpentinite and the sedimentary cover (Fig.6).

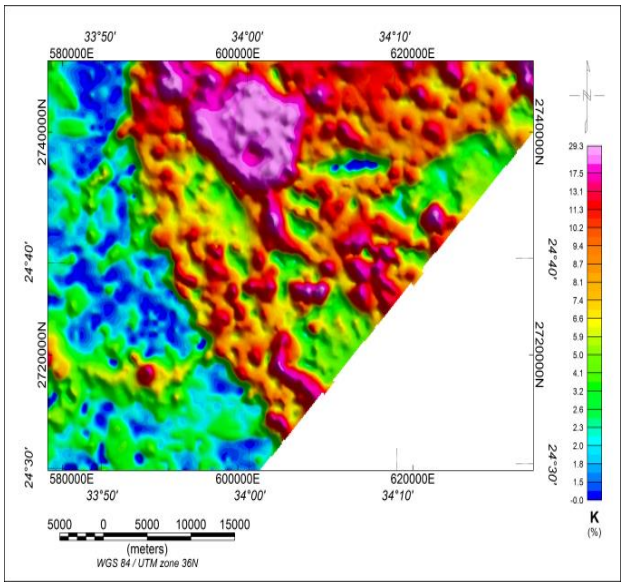

Fig. (6) Potassium map in %, of Hamash area, South Eastern Desert, Egypt

Ternary (Composite) Images

Ternary maps are color composite images made by modulating the red, green and blue in proportion to the radioelement concentration values of the K, eTh, eU, and their ratio grids. Subsequently, specific rock types frequently have characteristic ratios of the three radioactive elements; the ternary maps of these ratios are a suitable geological and mineral exploration tool for differentiating the zones of consistent lithology and contacts between different lithologies]10[. Two composite color image maps are present as follows:

1.Equivalent thorium composite image map eTh, eTh/eU and eTh/K

2.Potassium composite image map K, K/eTh, K/eU

Assigning a different primary color to each data set and then overlaying the outcomes produce these images. Using primary colors, the number of data sets that can be combined is limited to three. The three parameters must be given a definite primary color and the choice of whether high values of all three parameters will create dark colors (black) or light colors (white) must be made. The choice of which combination to use must take account of consideration of the purpose of the geophysical features of interest to the interpreter.

Equivalent thorium composite image map

Fig. (7) False colored equivalent thorium ternary image of Hamash area, South Eastern Desert, Egypt.

2 Potassium composite image map

The potassium composite image combines K (in red) with two ratios K/eTh (in green) and K/eU (in blue) (Fig. 8). This image highlights the relative distribution of potassium and emphasizes zones of potassic alteration. Outstanding to the map the high concentration of K is associated with Abu Aggag formation, Natash volcanics, Quaternary deposits, Dokhan volcanics, old granite, and ring complex (Fig. 8). The moderate values associated with younger granite, Post-Hammamat felsite, intermediate to acidic metavolcanics and metapyroclastics, and leucocratic medium to high-grade metamorphic rocks to low values in metagabbro to metadiorite (Fig. 8). The high concentration of K, K/eTh, K/eU is marked by the white color and generally, it is limited in three rock units they are younger granite, older granite, and gabbroic rocks. On the other hand, the low concentration of K, K/eTh, K/eU is marked by the dark color which characterized the Cretaceous formations (Abu Aggag formation, Umm Barmil formation, Taref formation, and Quseir formation) and ophiolitic serpentinite (Fig. 8). The high K/eTh and K/eU ratios appear in green and blue color which associated with the basement rocks of ophiolitic serpentinite and Dokhan volcanics. K/eU ratio has a moderate value noticed in intermediate to acidic metavolcanics and metapyroclastics and ophiolitic metagabbro and high value in Abu Aggag formation (Fig. 8)

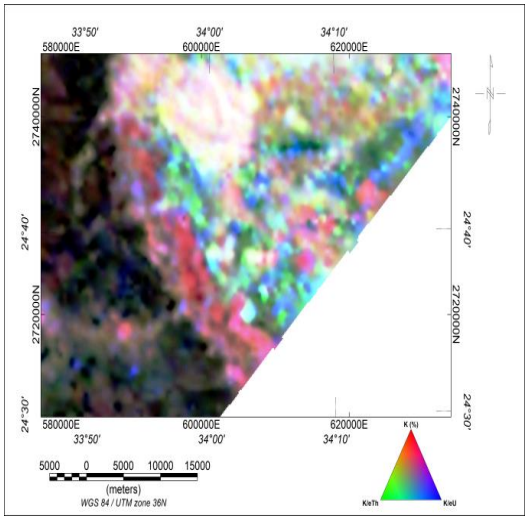

Fig. (8) False colored potassium ternary image of Hamash area, South Eastern Desert, Egypt

Conclusions

Airborne gamma-ray spectrometric data provide an excellent method for defining the radioactive zones at Hamash area (in the surveyed area) through the interpretation of radioelements and ternary images. The radioelement concentration values of the equivalent Uranium (eU), equivalent Thorium (eTh), and Potassium (K) successively discriminated several distinctive radioactive zones related to some rock unites in Hamash area. These rock units are younger granite, Post-Hammamat felsite, metagabbro to metadiorite, Natash volcanics, older granite, leucocratic medium to high-grade metamorphic rocks, trachyte plugs and sheets, and ring complex. Gamma-ray spectrometric data shows distinct values and responses for the alteration zones around the gold mines in the Hamash area and within different rock types which may be considered new host rocks of gold mineralization

References

1. Abd El Nabi, S.H. (2013), Role of γ-ray spectrometry in detecting potassic alteration associated with Um Ba'anib granitic gneiss and metasediments, G. Meatiq area, Central Eastern Desert, *Egypt. Arab. J. Geosci*, **6,** 1249-1261.
2. Aero Service (1984), Final operational report of airborne magnetic / radiation Survey in the Eastern Desert, Egypt. For the Egyptian General Petroleum Corporation, Cairo, Egypt. Aero Service, Houston. Texas, USA, six volumes.
3. Anderson, H., and Nash, C. (1997), Integrated lithostructural mapping of the Rossing area, Namibia using high resolution aeromagnetic, radiometric, Landsat data and aerial photographs. Explor. Geophys, **28,** 185-191.
4. Charbonneau, B.W., Holman, P.B., and Hetu, R.J. (1997), Airborne gamma spectrometer magnetic-VLF survey of northeastern Alberta. In: MacQueen (Ed.), Exploring for Minerals in Alberta: Geological Survey of Canada Geoscience Contributions, Canada-Alberta Agreement on Mineral Development. Geological Survey of Canada Bulletin, **500,** 107-132.
5. Chiozzi, P., Pasquale, V., and Verdoya, M. (1998), Ground radiometric survey of U, Th

and K on the Lipari Island, Italy. *Journal of applied geophysics*, **38(3),** 209-217.

6. Cook, S.E., Corner, R.J., Groves, P.R., and Grealish, G.J. (1996), Use of airborne gamma radiometric data for soil mapping. *Aust. J. Soil Res*, **34**, 183-194.
7. Coral, C. (1987), Geological Map of Egypt, Scale 1: 500,000,-NH36SW-Beni Suef, Egypt. The Egyptian General Petroleum Corporation, Cairo (EGPC), Egypt.
8. Dentith M., and Mudge S.T. (2014), Geophysics for the mineral exploration geoscientist. 1st edition, United States of America, Cambridge University Press, New York.
9. Dickson, B. L. (2004), Recent advances in aerial gamma-ray surveying. *Journal of Environmental Radioactivity***, 76(1-2),** 225-236.
10. Duval, J. S. (1983), Composite color images of aerial gamma-ray spectrometric data. Geophysics, **48(6),** 722-735.
11. El-Sadek, M.A. (2009), Radiospectrometric and magnetic signatures of a gold mine in *Egypt. J. Appl. Geophys***, 67,** 34-43.
12. Ford, K.L., Savard, M., Dessau, J.-C., Pellerin, E., Charbonneau, B.W., and Shives, R.B.K. (2000), The role of gamma-ray spectrometry in radon risk evaluation: a case history from Oka, Quebec. GeoCanada 2000 Abstracts CD-ROM.
13. Graham, D.F., and Bonham-Carter, G.F. (1993), Airborne radiometric data: a tool for reconnaissance geological mapping using a GIS. Photogramm. Eng. Remote. Sens**, 58 (8),** 1243-1249.
14. Grasty, R.L., and Shives, R.B.K. (1997), Applications of gamma-ray spectrometry to mineral exploration and geological mapping, Workshop presented at Exploration 97: Fourth Decennial Conference on Mineral Exploration.
15. Hyvönen, E., Turunen, P., Vanhanen, E., Arkimaa, H., and Sutinen, R. (2005), Airborne gamma-ray surveys in Finland. Geological Survey of Finland, Special Paper **39,** 119-134.
16. International Atomic Energy Agency (IAEA) (2010), Radioelement mapping. IAEA Nuclear Energy Series, No. NF-T-1.3, Vienna, Austria, 108.
17. Jaques, A.L., Wellman, P., Whitaker, A., and Wyborn, D. (1997), High-resolution geophysics in modern geological mapping. AGSO *Journal of Australian Geology and Geophysics*, **17 (2),** 159-174.
18. Lahti, M., Jones, D.G., Multala, J., and Rainey, M.P. (2001), Environmental applications of airborne radiometric surveys. Expanded Abstracts, 63rd Annual Conference, European Association of Geoscientists and Engineers.
19. Lo, B.H., and Pitcher, D.H. (1996), A case history on the use of regional aeromagnetic and radiometric data sets for lode gold exploration in Ghana. Annual Meeting Expanded Abstracts, Society of Exploration Geophysicists, 592-595.
20. Sanderson, D.C.W., Allyson, J.D., Tyler, A.N., and Scott, E.M. (1995), Environmental Applications of Airborne Gamma-Ray Spectrometry, Application of Uranium Exploration Data and Techniques in Environmental Studies. IAEA-TECDOC-827, IAEA, Vienna, 71-79.
21. Wilford, J.R., Bierwirth, P.N., and Craig, M.A. (1997), Application of airborne gamma-ray spectrometry in soil/regolith mapping and applied geomorphology. *AGSO J. Austral Geophys*, **17**, 201-216